Ford, L. R., *Differential Equations,* McGraw-Hill, New York (1955).

Ginn, R. F., and M. M. Denn, "Rotational Stability in Viscoelastic Liquids: Theory," *AIChE J.*, **15**, 450 (1969).

Hansen, R. J., and R. C. Little, "Pipe Diameter, Molecular Weight, and Concentration Effects on the Onset of Drag Reduction," *Chem. Eng. Progr. Symp. Ser. No. 111,* **67**, 93 (1971).

———., and Forame, P. C., "Experimental and Theoretical Studies of Early Turbulence," *Proc. First Pacific Congr. on Chem. Eng.*, Part 2, 306, Kyoto (1972).

Kusamizu, S., L. A. Holmes, A. A. Moore, and J. D. Ferry, "The Steady State Compliance of Polymer Solutions," *Trans Soc. Rheol.*, **12**, 559 (1968).

Little, R. C., and M. Wiegard, "Drag Reduction and Structural Turbulence in Flowing Polyox Solutions," *J. Appl. Polymer Sci.*, **14**, 409 (1970).

Lumley, J. L., "Applicability of the Oldroyd Constitutive Equation to Flow of Dilute Polymer Solutions," *Phys. Fluids,* **14**, 2284 (1971).

Meister, B. J., and R. D. Biggs, "Prediction of the First Normal Stress Difference in Polymer Solutions," *AIChE J.*, **15**, 643 (1969).

Metzner, A. B., J. L. White, and M. M. Denn, "Behavior of Viscoelastic Materials in Short-Time Processes," *Chem. Eng. Progr.*, **62**, 81 (1966).

Mook, D. T., "Stability of Parallel Flows of Second-Order Liquids," *Phys. Fluids,* **15**, 219 (1972).

Oldroyd, J. G., "On the Formulation of Rheological Equations of State," *Proc. Roy. Soc. London, A200* 523 (1950).

Paterson, R. W., and F. H. Abernathy, "Transition to Turbulence in Pipe Flow for Water and Dilute Solutions of Polyethylene Oxide," *J. Fluid Mech.*, **51**, 177 (1972).

Pekeris, C. L., "Stability of the Laminar Flow Through a Straight Pipe of Circular Cross-Section to Infinitesimal Disturbances which are Symmetric about the Axis of the Pipe," *Proc. Nat. Acad. Sci.*, **34**, 285 (1948).

Platten, J., and R. S. Schechter, "Stability of the Flow of a Slightly Viscoelastic Fluid," *Phys. Fluids,* **1**, 832 (1970).

Ram, A., and A. Tamir, "Structural Turbulence in Polymer Solutions," *J. Appl. Polymer Sci.*, **8**, 2751 (1964).

Romanovskaya, I. L., and N. M. Khalfina, "On the Asymptotic Behavior of Confluent Functions," *U.S.S.R. Comp. Math. Math. Phys.*, **7**, 661 (1967).

Salwen, H., and C. E. Grosch, "The Stability of Poiseuille Flow in a Pipe of Circular Cross Section," *J. Fluid Mech.*, **54**, 93 (1972).

Schensted, I. V., "Contributions to the Theory of Hydrodynamic Stability," Tech. Report of College of Eng., Univ. Michigan, Ann Arbor (1960).

Slater, L. J., *Confluent Hypergeometric Functions,* Cambridge Univ. Press, Cambridge (1960).

Spielberg, K., and H. Timan, "On Three and Two-Dimensional Disturbances of Pipe Flow," *J. Appl. Mech.*, **27** 381 (1960).

Watson, G. N., *Theory of Bessel Functions,* Cambridge University Press, Cambridge (1945).

White, J. L., and A. B. Metzner, "Development of Constitutive Equations for Polymeric Melts and Solutions," *J. Appl. Polymer Sci.*, **7** 1867 (1963).

Manuscript received May 5, 1972; revision received October 11, 1972; paper accepted October 16, 1972.

Liquid-Liquid Contacting in Unbaffled, Agitated Vessels

Drop size and dispersed-phase holdup were measured for liquid dispersions in covered, unbaffled agitated vessels with no gas-liquid interface and hence no vortex for batch and continuous flow. Vessel diameters of 0.245 and 0.372 m, turbine impellers of diameters 0.0762 and 0.127 m in two locations, four organic- and three water-dispersed systems of a wide range of properties, and a wide range of operating conditions were studied. The data for average drop diameter and dispersed-phase holdup, from which specific interfacial area may be computed, were successfully correlated through modification of the theories of maximum drop size in an isotropically turbulent fluid.

BRUCE WEINSTEIN
and ROBERT E. TREYBAL

Department of Chemical Engineering
New York University
New York, New York 10453

SCOPE

Vessels for mechanical agitation of liquids in most processes are usually operated batchwise and open to the air with an air-liquid surface, commonly with a rotating impeller on an axially arranged shaft. Under these conditions, unless the vessel is suitably baffled, a vortex will form at all but the lowest agitator speeds. Rushton (1951) has shown that when a vortex forms, it is impossible to scale up the power requirement for agitation, even with geometrically similar vessels. Since the vortex can be eliminated by introducing four wall baffles (Mack and Kroll, 1948), almost all subsequent work with agitated vessels has been done with baffles installed.

In liquid-liquid extraction operations, two immiscible liquids are vigorously agitated so as to disperse one of them into tiny droplets of large interfacial area. Since one of the liquids is invariably organic, it is desirable to operate the agitated vessel covered; and since the operations usually require continuous flow of the liquids, it is easy to operate the vessel completely filled with liquid,

---

Bruce Weinstein is with Charles Ross and Sons, Hauppauge, N. Y.

that is, with no air-liquid interface. Under these conditions, there is no vortex even in the absence of baffles. Furthermore, Laity and Treybal (1957) have shown that for such vessels power characteristics can be scaled up for agitation of either single- or two-phase liquid systems.

There is a growing accumulation of evidence that unbaffled vessels operate more efficiently, that is, with less power for the same result, than do baffled vessels, and they thus become very attractive, particularly if the vortex is eliminated. For example, the rate of catalytic hydrogenation of dinitrotoluene in solution is substantially larger in the absence of baffles than with baffles (Greenfield, 1969). When such vessels are used to carry out second-order, competitive-consecutive, liquid-phase reactions, the power required to attain specified yields is substantially less without baffles (Paul and Treybal, 1971). In the case of continuous liquid extraction in the absence of an air-liquid interface, Overcashier et al. (1956) show substantially higher stage efficiencies for the same agitation power in the absence of baffles; the continuous-phase mass-transfer coefficients are similarly substantially larger in the absence of baffles (Schindler and Treybal, 1968; Mok and Treybal, 1971), and these phenomena have been attributed to the greater coalescence-redispersion frequency for the drops in the absence of baffles.

For purposes of design of liquid-extraction equipment, we need to know not only the mass-transfer coefficients but also the interfacial area. There is a large accumulation of data for baffled vessels but only a few limited measurements of area in unbaffled vessels (Fick et al., 1954; Mok and Treybal, 1971; Rea and Vermeulen, 1953; Schindler and Treybal, 1968), and these are insufficient. This paper reports a detailed study of drop size and dispersed-phase holdup, from which interfacial area can be calculated, in unbaffled vessels operated batch-wise and with continuous flow, with no air-liquid interface and no vortex, for a wide range of fluid properties, flow rates, and ratio of immiscible liquids, impeller speeds, two vessel sizes, and two impeller sizes and locations. These data are necessary for estimating stage efficiencies.

CONCLUSIONS AND SIGNIFICANCE

The study included seven liquid-liquid systems formed from four pairs of organic-aqueous phases of a wide range of physical properties. The variation of interfacial area, measured by light transmittance, and dispersed-phase holdup with location in the vessel was determined, and vessel-average values of these and the mean drop diameters were computed.

The drop-size data were successfully correlated, through modification of Hinze's (1955) theory of the maximum drop size in an isotropically turbulent fluid, by remarkably simple equations of the form

$$\bar{d}_p = 10^{c_1+c_2\bar{\Phi}}\,\nu_C{}^{c_3}\,\epsilon^{c_4}\left(\frac{\sigma g_c}{\rho_C}\right)^{c_5}$$

with separate values of the constants for batch and continuous flow. These equations can be put in the form of Weber numbers

$$N_{We} = \rho_C\,\overline{u^2}\,\bar{d}_p/\sigma g_c = 10^{\overline{c_6+c_7\Phi}}$$

and the expressions for $\overline{u^2}$ required for this are shown to be characteristic of scales of turbulence for eddies lying between those in the inertial subrange, sometimes also referred to as the Kolmogoroff range, and those in the energy-dissipation range. Correlations were also obtained for the dispersed-phase holdup for continuous flow. The interfacial area can be computed from these.

Comparison with a corresponding correlation for baffled vessels leads to the tentative conclusion that for otherwise equal conditions the interfacial area in baffled and unbaffled vessels is the same at equal impeller power per unit volume of vessel contents. It is apparently the larger mass transfer coefficients, rather than interfacial area, which accounts for the higher extraction stage efficiency in unbaffled as compared with baffled vessels.

The new correlations represent essentially the only such information for unbaffled vessels, and they also cover a range of conditions exceeding any thus far reported for baffled vessels. They provide information essential to the interpretation of the mass-transfer characteristics of unbaffled vessels used for liquid extraction, and to the design of such vessels.

The detailed studies of interfacial area and drop size for liquid-liquid dispersions in agitated vessels have all been limited to baffled vessels, and with few exceptions to batch operation. Space limitations preclude a complete review. Only the relatively recent studies have considered the variation with location of such things as drop size, specific area, and the like. From these something of the scope of the problem can be gleaned. A variety of techniques has been used, and it is uncertain what influence the technique has on the observed phenomena.

Although we do not have the detailed dependencies on conditions, it is known that drop size varies with location in both baffled vessels (Calderbank, 1958; Mlynek and Resnick, 1972; Mok and Treybal, 1971; Schindler and Treybal, 1968), and in unbaffled vessels (Mok and Treybal; Schindler and Treybal). The drop size at any location in baffled and unbaffled vessels is not uniform (Chen and Middleman, 1967; Kawecki et al., 1967; Schindler and Treybal, 1968; Sprow, 1967; Sullivan and Lindsay, 1962), and is influenced by flow rate (Bouyatiotis and Thornton, 1963, 1967; Mok and Treybal, 1971; Schindler and Treybal, 1968). The dispersed-phase holdup, that is, drop concentration, varies with location (Mok and Treybal; Schindler and Treybal). During continuous operation at all but very high impeller speeds, the average dispersed-phase holdup in baffled vessels is less than the fraction of dispersed phase in the combined feeds, at least if the dispersed phase has the smaller density and the flow is upward (Bouyatiotis and Thornton, 1963, 1967; Treybal, 1963). A detailed study of unbaffled vessels must consider these phenomena.

The following definitions are useful. The Sauter-mean drop diameter is the uniform diameter which provides the same volume/area as is actually present in a dispersion of nonuniform drop diameters. The local value is d_p

$$d_p = \sum_{\text{all } i} n_i d_i^3 \Big/ \sum_{\text{all } i} n_i d_i^2 \qquad (1)$$

The local dispersed-phase holdup and specific interfacial area are φ and a, respectively. The vessel-average of these are $\overline{d}_p$, $\overline{\varphi}$, and $\overline{a}$, and the relationships among them are

$$a = 6\,\varphi/d_p; \quad \overline{a} = 6\,\overline{\varphi}/\overline{d}_p \qquad (2)$$

The vessel-average values have the greater utility in extractor design.

APPARATUS AND PROCEDURES

A detailed description is available elsewhere (Weinstein, 1972). Two mixing vessels (Figure 1) were used, each constructed of a Pyrex glass cylinder closed with stainless-steel end plates. The lower plate of the smaller vessel contained a circular glass window, flush inside, through which the dispersion could be photographed. The upper plate, made with a slight taper to facilitate removal of air while filling, contained a large opening fitted with a vertical chimney for introducing a light-transmittance probe and a sampling thief. The port was nearly closed by a close-fitting plate, flush with the top of the vessel, through which those devices passed, thus preventing entry of air into the vessel. The liquids to be contacted were pumped separately into the bottom of the vessel at rates measured by Rotameters; the dispersion left at the top and passed to a 0.45-m^3 (120 gal.) stainless-steel continuous settler. The settled liquids were then circulated back to the mixing vessel. The liquids came into contact only with stainless steel, glass, and Teflon.

The geometrically similar, 6-bladed flat-blade turbine impellers were located on the axes of the vessels, centrally as in Figure 1 and also at $H/3$ from the bottom. The circular plates upon which the blades of the turbines are fastened are $D/1.5$ in diameter, and the blades are $D/5 \times D/4$. The combination of smaller impeller in the smaller vessel, with larger impeller in the larger vessel at a similar location, provided essentially geometrically similar configurations.

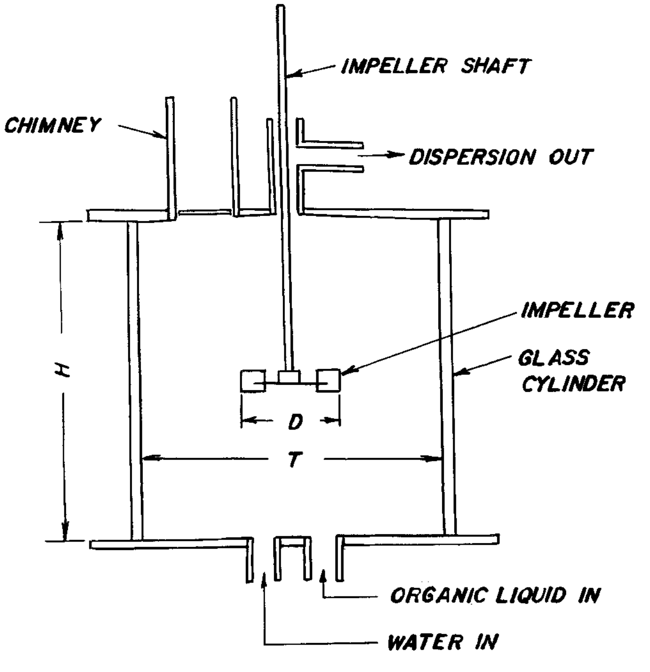

VESSEL	H, m	T, m	D, m (in.)
SMALL	0.245	0.245	0.0762, 0.127 (3,5)
LARGE	0.382	0.372	0.127 (5)

Fig. 1. Agitated vessels, schematic.

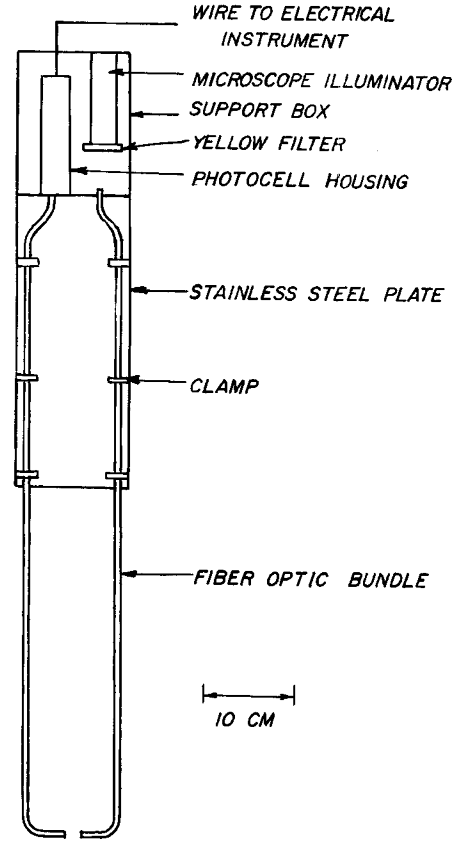

Fig. 2. Light-transmittance probe.

The specific interfacial area was measured by the light-transmittance technique (Rodger, 1956; Trice and Roger, 1956; Schindler and Treybal, 1968; Mok and Treybal, 1971). In this case the light probe was made of two fiber-optic light pipes especially made by Bausch and Lomb, Inc. Refer to Figure 2. Each light pipe consisted of a bundle of many glass light wires encased in 9.52-mm diam. stainless steel tubing. Both the tube for admitting light and that for collecting it, rigidly clamped relative to each other, entered from the top through the plate previously described, and the dispersion gap was 14.3 mm. The probe could be moved about in the vessel, within limits, for exploration. The electronic circuitry for amplifying the photo-cell output was similar to that of Rodger (1956). In order to calibrate the device, photographs were taken through the window in the bottom of the smaller vessel, using the same camera and techniques described in detail earlier (Schindler and Treybal, 1968). Photographs of the dispersion were taken while the gap between the light pipes was located at the extreme bottom of the vessel. During these measurements the vessel was operated batch-wise with mutually saturated liquids. Each photograph showed the image of a hypodermic tube mounted on the upper side of the glass window to establish a length standard. The developed film was projected onto a screen and when the drop-size distribution was obtained, an interfacial area was computed and related to the photocell current. Calibration was necessary for each combination of dispersed and continuous liquid. In each case, graphs resembling those of Schindler and Treybal resulted. As with all light-transmittance techniques, indeed with all available techniques, there is no way of assessing the influence of the method of measurement or the instrument used. The present probe has less bulk than others that have been used and should have caused a minimum of disturbance.

Dispersed-phase holdup was measured at the same locations as the light-transmittance measurements by withdrawing a 250-ml sample of the vessel contents. Local mean drop diameters were then computed from the specific area and holdup with Equation (2). Light-transmittance and dispersed-phase holdup measurements for each system were made at locations for two of the vessel arrangements as shown in Figure 3 and for other arrangements in similar locations.

Four pairs of organic liquids with water were studied, in each case with organic liquid both continuous and dispersed, making eight systems in all. The laboratory distilled water and commercial grade (99+ wt. % pure) organic liquids were used. All experiments were conducted with mutually saturated liquids, and there was therefore no mass transfer. Temperatures ranged from 24°C to 31°C, for which detailed property data were obtained; an abbreviated list of properties is shown in Table 1. Table 2 lists the range of conditions studied.

EXPERIMENTAL RESULTS

Complete tabulations of all experimental data for 818 runs are available elsewhere (Weinstein, 1972). It was impossible completely to disperse water in isopropyl benzene at the upper limit of impeller speeds available, 10.33 rev/s and data for this combination are not further discussed. Data for water dispersed in methylamyl acetate are anomalous, and these also are omitted from the discussion which follows.

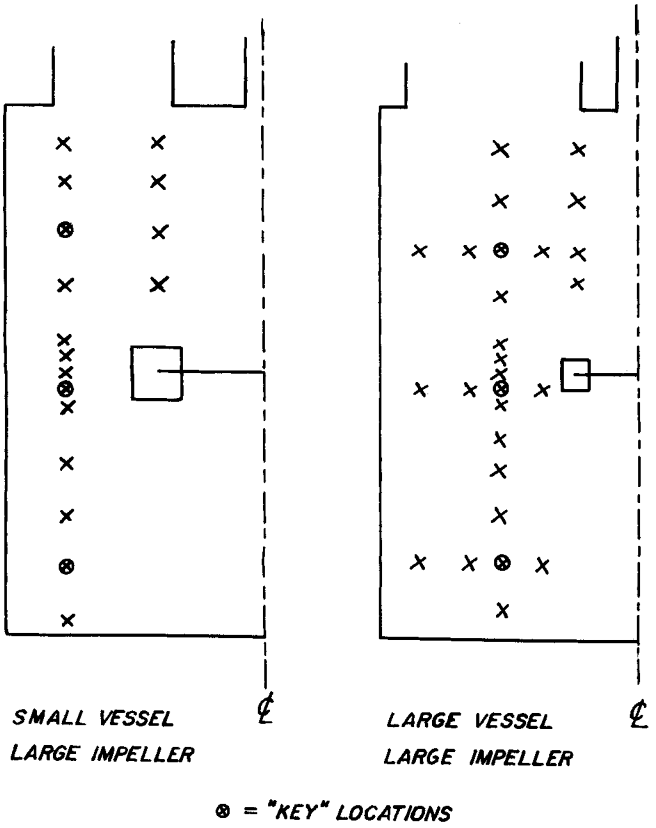

Fig. 3. Measurement points for centrally located impeller. Measurements made at points marked X.

Local values of dispersed-phase holdup, mean drop size, and specific area all vary with location in the vessel; Figure 4 shows an example of this for a particular set of conditions. Dispersed-phase holdup tends to be larger at the top of the vessel for cases where $\rho_D < \rho_C$ and larger at the bottom when $\rho_D > \rho_C$. It becomes more uniform throughout the vessel at higher impeller speeds for lower values of density difference of the liquids, and when the impeller is at the lower position. Generally, the nature of the variation of φ with location is relatively independent of flow rate. Nevertheless, at very high flow rates of the dispersed liquid and lower impeller speeds, the feed stream penetrates several centimeters into the vessel before being dissipated, and φ is then lower near the bottom of the vessel and higher near the top, as compared with values for batch operation. The effect, however, is not large.

Drop diameters are invariably smallest in the vicinity of the impeller. In the impeller discharge stream, drop size increases as radial distance from the impeller increases, owing to coalescence. At a radial distance from the impeller top of about 6.5 cm, the drop diameters are about the same as those in the bulk of the vessel volume.

Generally, the shape of curves such as those of Figure 4 depend upon impeller speed, liquid properties, vessel geometry, and to a lesser extent, upon flow rate. Except in the immediate vicinity of the impeller, d_p, φ, and a are practically independent of radial position.

Vessel-average values of the dispersion properties are of greatest value; these may be estimated from curves such as those in Figure 4. Such detailed explorations, from measurements at points marked X in Figure 3, were made for each system studied. But in order to reduce the time required, measurements for most of the runs were taken at key locations, such as those marked in Figure 3, where the measured φ and a could be used to compute accurate vessel-average values $\overline{\varphi}$ and $\overline{a}$. The detailed pro-

TABLE 1. SYSTEM PROPERTIES AT 25°C

Saturated liquid solvent/solute	Density, kg/m³ = (g/cm³) (1000)	Viscosity N · s/m² = centip/ 1000	Interfacial tension, N/m = (dynes/cm)/ 1000
Cyclohexanone/water	946	0.002015	0.00376
Water/cyclohexanone	996	0.001146	
Octanol/water	831	0.00743	0.0102
Water/octanol	996	0.000902	
Methylamyl acetate/water	857	0.000863	0.0166
Water/methylamyl acetate	997	0.000892	
Isopropyl benzene/water	856	0.000722	0.0360
Water/isopropyl benzene	996	0.000896	

TABLE 2. RANGE OF CONDITIONS

Vessel	Impeller diam., m	Impeller speed, rev./s	Flow rate total liquid m³/s × 10⁴	Dispersed-phase fraction of total feed[b]	Avg. dispersed phase holdup, $\overline{\varphi}$	Avg. drop diam., $\overline{d}_p$, m × 10⁴	Avg. specific interface area, $\overline{a}$, m²/m³
Small	0.0762[c]	5.0-10.33	0-3.785[a]	0.125-0.833	0.079-0.593	2.32-8.44	991-6560
Small	0.127[d]	2.5-5.33	0-3.785	0.125-0.833	0.090-0.512	2.21-6.74	1253-7255
Large	0.127	4.17-5.33	0-3.785	0.125-0.500	0.079-0.496	2.72-6.95	1204-6002

[a] 6 gal/min.
[b] Continuous flow.
[c] 3 in.
[d] 5 in.

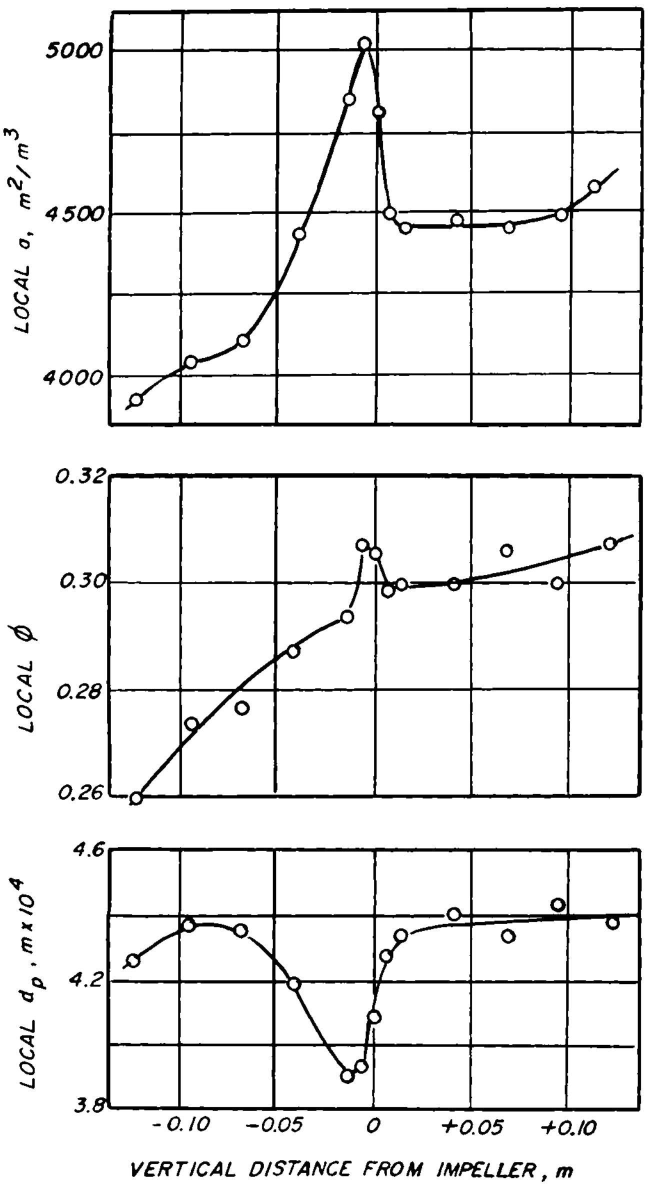

Fig. 4. Influence of vertical position. Octanol dispersed in water, batch, small vessel, small impeller rotating at 6.67 rev/sec

cedure for this is described elsewhere (Weinstein, 1972). No data could be taken directly under the impeller, and average values as calculated in this manner are assumed to be valid for this region. The vessel-average $\overline{d_p}$ was then computed through Equation (2).

CORRELATION OF THE DATA

The data were successfully correlated by modification of Hinze's concept of the mechanism of the splitting of drops in isotropically turbulent fluids. Upon consideration of the forces acting upon isolated liquid drops immersed in the turbulent fluid, Hinze (1955) obtained

$$N_{We,C} = \rho_C \overline{u^2}\, d_{\max}/\sigma g_c = \text{constant} \qquad (3)$$

as the minimum value of N_{We} when drop breakage occurs, on the assumption that N_{vis} is small relative to unity. When computed with $\overline{d_p}$, our values of N_{vis} lie in the range 0.0045 to 0.1495, which is taken to be suitably small. Figure 5 is a representation of the energy-spectrum function for eddies in a turbulent fluid. For drops of a size similar to eddy wave lengths in the inertial subrange (Hinze, 1959),

$$\overline{u^2} = C_1(\epsilon\, d_{\max})^{2/3} \qquad (4)$$

and, if $\overline{d_p}$ is taken proportional to $d_{\max}$ for any particular drop-size distribution, then substitution into Equation (3) produces

$$\overline{d_p} = C_2\, \epsilon^{-2/5}(\sigma g_c/\rho_C)^{3/5} \qquad (5)$$

Now, Cutter (1966) reported the scale of turbulence for the energy-containing eddies in the impeller-discharge stream of an agitated, baffled vessel, which may be approximated by (Schwartzberg and Treybal, 1969)

$$\frac{1}{k_e} = L_e = 0.08\, D \qquad (6)$$

The scale of energy-dissipating eddies is (Hinze, 1959)

$$\frac{1}{k_d} = \eta = (\nu_C^3/\epsilon)^{1/4} \qquad (7)$$

Our values of $\overline{d_p}$ are in the range 2.21 × 10^{-4} to 8.44 × 10^{-4} m, while our L_e = 61 × 10^{-4} to 102 × 10^{-4} m, and our η = 0.36 × 10^{-4} to 3.2 × 10^{-4} m. Therefore our drops are probably similar in size to eddies in the wave-number range between the inertial subrange and the energy-dissipation range.

The universal equilibrium range includes the initial subrange and all larger wave numbers, and Heisenberg's (1948) spectrum function may be assumed. For wave numbers near the dissipation range, it can be simplified and integrated (Weinstein, 1972) to yield

$$\overline{u^2} = C_3\, \nu_C^{-4}\, \epsilon^2\, \overline{d_p}^6 \qquad (8)$$

This, with $\overline{d_p}$ instead of $d_{\max}$ in the definition of N_{We}, produces

$$\overline{d_p} = C_4\, \nu_C^{4/7}\, \epsilon^{-2/7}(\sigma g_c/\rho_C)^{1/7} \qquad (9)$$

Since our $\overline{d_p}$ lie in a range of wave numbers between those of the inertial subrange and the dissipation range, an empirical expression for $\overline{u^2}$ is needed. This is taken to be

$$\overline{u^2} = \gamma\, \nu_C^{c'_1}\, \epsilon^{c'_2}\, \overline{d_p}^{c'_3} \qquad (10)$$

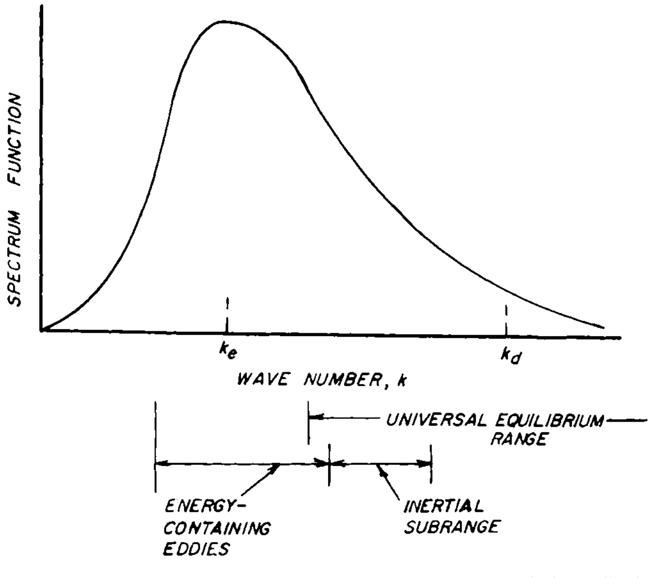

Fig. 5. Energy-spectrum function for eddies in a turbulent fluid, after Hinze (1959).

TABLE 3. DROP DIAMETERS FOR BATCH OPERATION

Circumstance	Equation	Equation	Avg. dev., %	Max. dev., %
All data	$\overline{d}_p = 10^{(-2.316 + 0.672\overline{\phi})} \nu_C^{0.0722} \epsilon^{-0.194} (\sigma g_c/\rho_C)^{0.196}$ $N_{We} = 10^{(-10.09 + 3.428\overline{\phi})}$ $\overline{u^2} = \gamma \nu_C^{-0.368} \epsilon^{0.990} \overline{d}_p^{4.103}$	(13*a*)	7.04[a] 8.75[b]	26.7[a] 28.6[b]
Both vessels $\frac{D}{T} \doteq \frac{1}{3}$	$\overline{d}_p = 10^{(-2.488 + 0.714\overline{\phi})} \nu_C^{0.0700} \epsilon^{-0.213} (\sigma g_c/\rho_C)^{0.171}$ $N_{We} = 10^{(-12.20 + 4.172\overline{\phi})}$ $\overline{u^2} = \gamma \nu_C^{-0.409} \epsilon^{1.246} \overline{d}_p^{4.841}$	(13*b*)	5.74[a]	20.4[a]
Small vessel $\frac{D}{T} \doteq \frac{1}{2}$	$\overline{d}_p = 10^{(-1.645 + 0.587\overline{\phi})} \nu_C^{0.100} \epsilon^{-0.253} (\sigma g_c/\rho_C)^{0.298}$ $N_{We} = 10^{(-4.802 + 1.967\overline{\phi})}$ $\overline{u^2} = \gamma \nu_C^{-0.335} \epsilon^{0.850} \overline{d}_p^{2.354}$	(13*c*)	5.72[a]	31.4[a]

[a] Impeller centrally located.
[b] Impeller in lower position.

which can revert to Equation (4) (with $\overline{d}_p$ instead of $d_{\max}$) or to Equation (8) with certain values of the exponents. In combination with the definition of N_{We}, there is obtained for isolated drops

$$\overline{d}_p = C_5 \, \nu_C^{c'_4} \, \epsilon^{c'_5} (\sigma \, g_c/\rho_C)^{c'_6} \tag{11}$$

The systems of the present work differ from that of Hinze in that swarms of drops were present, and there is an observable effect of drop concentration, or φ. The drops in the swarm discharged by the impeller stream have the statistical-average stable size for a turbulent field corresponding to the local energy-dissipation rate. If φ were very small (say of the order of 0.01), then while drops traversed the bulk region of the vessel there would be very few drop collisions and coalescences, so that $\overline{d}_p$ *would* then be characteristic of the energy-dissipation ratio at the impeller. But in this work, $\varphi = 0.08$ to 0.60, and collisions and coalescences are frequent—at a rate which increases as φ increases. In order to account for this influence of φ, Equation (11) was therefore modified by introducing various functions of φ of which the most successful empirically is

$$f_1(\overline{\varphi}) = 10^{c'_7 + c'_8 \overline{\phi}} \tag{12}$$

Equation (11) becomes, upon inclusion of Equation (12),

$$\overline{d}_p = 10^{c_1 + c_2 \overline{\phi}} \, \nu_C^{c_3} \, \epsilon^{c_4} (\sigma \, g_c/\rho_C)^{c_5} \tag{13}$$

for which the constants were determined from the data by a least-squares fit.

BATCH OPERATION

It has already been pointed out that $\overline{d}_p$ is nearly characteristic of the drop size in the bulk region of the vessel. Local values of ϵ and $\overline{u^2}$ vary with location, and Cutter (1966), for example, indicated that for baffled vessels vessels as much as 75% of the power input may be dissipated in the vicinity of the impeller. For unbaffled vessels, the energy-dissipation rate characteristic of the bulk region will be some unknown fraction of

$$\epsilon = \frac{P \, g_c}{V(1 - \overline{\varphi}) \rho_C} \tag{14}$$

and the unknown fractions will be incorporated in the coefficient of Equation (11). Values of P were computed from the correlation of Laity and Treybal (1957).

Results are shown in Table 3 in the form of Equation (13) and also expressed as the dimensionless N_{We}. In addition, equations for the corresponding $\overline{u^2}$ are included to show that the exponents lie between the values characteristic of the inertial subrange and the energy-dissipation range of the eddies. The effect of impeller location at least for the two positions studied is inconsequential.

CONTINUOUS FLOW

For the flow rates used in this work, the times of residence of the dispersed phase in the vessel were from 9.9 to 251 sec. For batch operation, it was observed that the steady state drop size usually required an agitation time of from 300 to 600 sec., with smaller values for larger values of impeller power. The implication is that $\overline{d}_p$ should be larger for continuous flow than for batch operation, to an extent depending upon the residence time.

When the dispersed liquid enters the vessel, it is rapidly broken down to globules that are several times larger (say 4 to 10 times) than the average steady state $\overline{d}_p$ for flow conditions. Only eddies of a size comparable to $\overline{d}_p$ cause breakage; larger eddies merely carry the globules along and smaller eddies do not contain sufficient energy. Whatever the breakage mechanism, the time required for final breakage of the globules should be inversely related to the frequency of the eddies of size $\overline{d}_p$, in turn directly related to $\overline{d}_p$ and hence to σ. An increase in interfacial tension should increase the time required for the feed stream to attain steady state drop size, and for otherwise equal circumstances, the ratio $\overline{d}_p(\text{flow})/\overline{d}_p(\text{batch}$ should be larger for larger σ. Figures 6 to 8 demonstrate this: for a system of very low interfacial tension, the effect of flow rate on $\overline{d}_p$ is negligible, but the influence becomes increasingly strong as the tension increases, somewhat moderated by higher impeller speeds.

The effect of residence time can be accounted for by modification of Equation (13), replacing $f_1(\overline{\varphi})$ with

$$f_2(\overline{\varphi}, t_D) = 10^{c'_7 + c'_8 \overline{\phi} + c'_9 t_D}$$

and correlations of this sort were developed. Actually, $\overline{\varphi}$ and t_D are functionally related, and better correlations were obtained by eliminating t_D and using Equation (13) for $\overline{d}_p$, together with a separate correlation for $\overline{\varphi}$.

For batch operation, all the impeller power is dissipated in the vessel. For flow operation, some of the impeller power is removed in the form of surface energy in the drops leaving with the effluent dispersion. The total rate of flow of interfacial surface in the effluent is $6 \, Q_D/\overline{d}_p$, and the corresponding power is

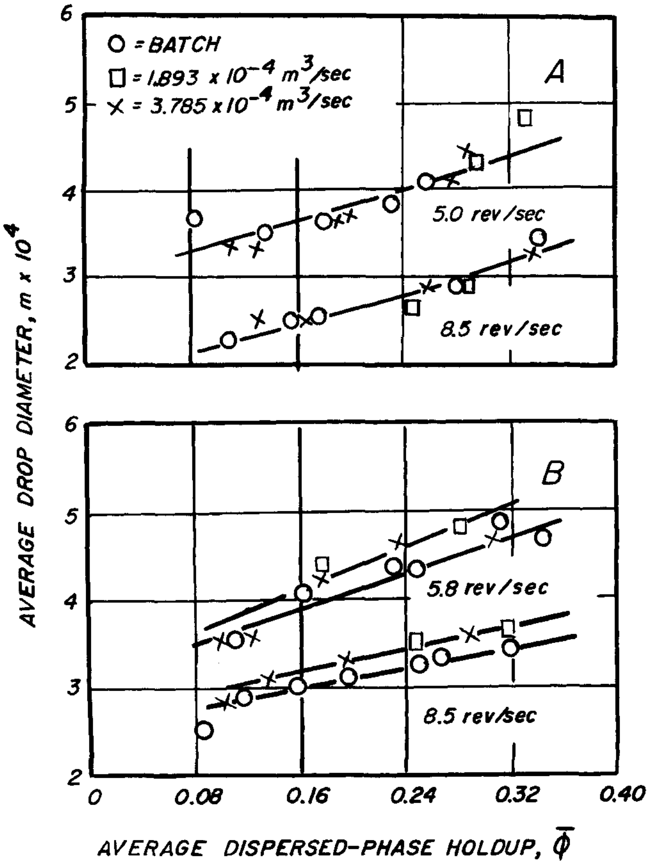

Fig. 6. Influence of flow rate. small vessel, small impeller: A, cyclohexane dispersed in water, interfacial tension = 3.76 dynes/cm; B, octanol dispersed in water, interfacial tension = 10.2 dynes/cm.

$$P_D = 6\,Q_D\sigma/\overline{d}_p \qquad (14)$$

The energy-dissipation rate for continuous flow is then

$$\epsilon = \frac{(P - P_D)g_c}{V(1-\varphi)\rho_C} \qquad (15)$$

In most cases P_D was between 1 and 3% of P, never greater than 6%. P was calculated from the correlation of Laity and Treybal (1957).

Energy also entered the vessel in the form of kinetic energy of the feed streams and left as kinetic energy of the effluent. The net input of energy from this source was negligible.

With respect to dispersed-phase holdup, as with baffled vessels, so with unbaffled vessels: the average $\overline{\varphi}$ is different from that corresponding to the fraction that the dispersed liquid represents of the toal feed. Owing to a lack of information on the fluid dynamics of unbaffled vessels, it was not found possible satisfactorily to develop a theoretical approach for describing $\overline{\varphi}$. An empirical approach was therefore adopted, using standard dimensional analysis:

$$N_\phi = C_6\, N_{Pv}{}^a\, N_F{}^b\, N_\rho{}^c\, N_G{}^d\, N_\mu{}^e \qquad (16)$$

The results are shown in Table 4 for $\overline{d}_p$ and in Table 5 for $\overline{\varphi}$. As with batch operation, the exponents in the expression for $\overline{u^2}$ lie between values corresponding to the inertial subrange and the energy-dissipation range for the eddies. In the case of $\overline{\varphi}$, separate correlations are necessary for dispersed phase lighter and heavier than the continuous phase, respectively.

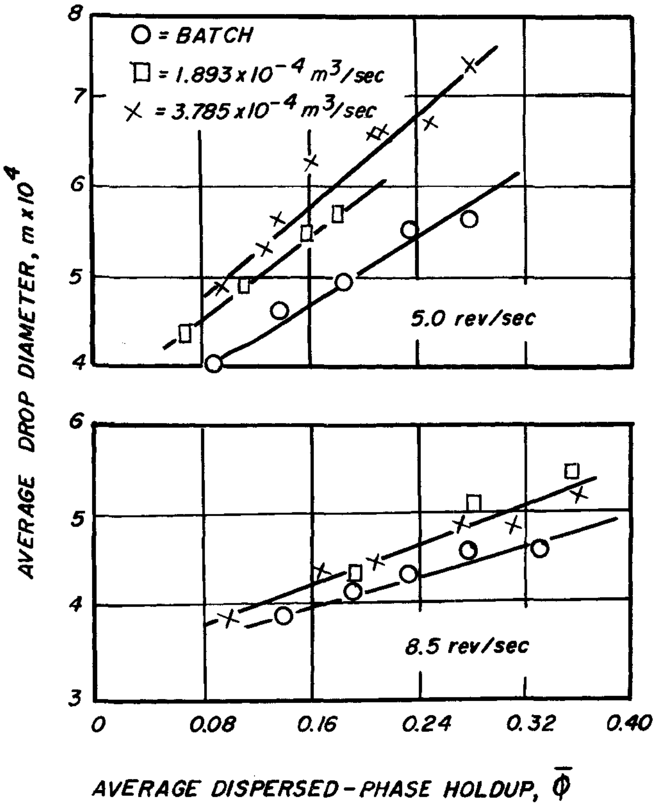

Fig. 7. Influence of flow rate, small vessel, small impeller: methylamyl acetate dispersed in water, interfacial tension = 16.6 dynes/cm.

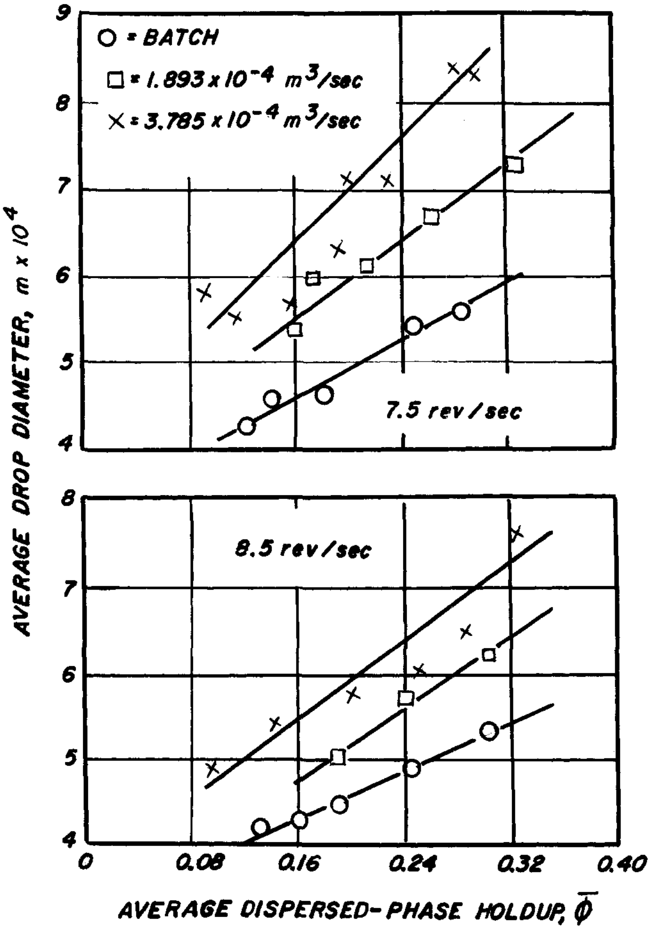

Fig. 8. Influence of flow rate, small vessel, small impeller: isopropylbenzene dispersed in water, interfacial tension = 36.0 dynes/cm.

TABLE 4. DROP DIAMETER FOR CONTINUOUS FLOW

Circumstance	Equation	Equation	Avg. dev., %	Max. dev., %
All data	$\overline{d_p} = 10^{(-2.066 + 0.732\overline{\phi})} \nu_C^{0.047} \epsilon^{-0.204} (\sigma g_c/\rho_C)^{0.274}$	(13*d*)	7.29[a]	32.5[a]
	$N_{We} = 10^{(-6.614 + 2.673\overline{\phi})}$		10.1[b]	28.6[b]
	$\overline{u^2} = \gamma \nu_C^{-0.173} \epsilon^{0.746} \overline{d_p}^{2.650}$			
Both vessels	$\overline{d_p} = 10^{(-2.192 + 0.765\overline{\phi})} \nu_C^{0.0344} \epsilon^{-0.192} (\sigma g_c/\rho_C)^{0.263}$	(13*e*)	7.69[a]	29.9[a]
$\frac{D}{T} \doteq \frac{1}{3}$	$N_{We} = 10^{(-7.303 + 2.909\overline{\phi})}$			
	$\overline{u^2} = \gamma \nu_C^{-0.131} \epsilon^{0.730} \overline{d_p}^{2.802}$			
Small vessel	$d_p = 10^{(-1.759 + 0.649\overline{\phi})} \nu_C^{0.0706} \epsilon^{-0.247} (\sigma g_c/\rho_C)^{0.304}$	(13*f*)	5.12[a]	26.4[a]
$\frac{D}{T} \doteq \frac{1}{2}$	$N_{We} = 10^{(-5.122 + 2.133\overline{\phi})}$			
	$\overline{u^2} = \gamma \nu_C^{-0.232} \epsilon^{0.812} \overline{d_p}^{2.288}$			

[a] Impeller centrally located.
[b] Impeller in lower position.

TABLE 5. DISPERSED-PHASE HOLDUP FOR CONTINUOUS UPWARD FLOW

Circumstance	Equation	Avg. dev., %	Max. dev., %
$\rho_D < \rho_C$ All data	$N_\phi = 10^{0.530} N_{Pv}^{0.247} N_F^{-0.427} N_\rho^{-0.430} N_G^{-0.401} N_\mu^{0.0987}$	11.3[a] 12.5[b]	64.2[a] 55.4[b]
Both vessels $\frac{D}{T} \doteq \frac{1}{3}$	$N_\phi = 10^{0.753} N_{Pv}^{0.284} N_F^{-0.480} N_\rho^{-0.396} N_G^{-0.449} N_\mu^{0.0927}$	9.92[a]	44.0[a]
Small vessel $\frac{D}{T} \doteq \frac{1}{2}$	$N_\phi = 10^{1.963} N_{Pv}^{0.301} N_F^{-0.416} N_\rho^{0.231} N_G^{-0.304} N_\mu^{-0.0410}$	9.20[a]	22.0[a]
$\rho_D > \rho_C$ All data	$N_\phi = 10^{0.703} N_{Pv}^{-0.131} N_F^{-0.0752} N_\rho^{-0.0677} N_G^{0.0299} N_\mu^{0.0949}$	4.35[a] 4.58[b]	12.2[a] 12.68[b]

[a] Impeller centrally located.
[b] Impeller in the lower position.

ANOMALOUS SYSTEMS

None of the correlations include data for the system water dispersed in methylamyl acetate, although data for the ester dispersed in water are included. The drops in both cases would be anticipated to be about the same size, in view of the physical properties but for water dispersed $\overline{d_p}$ was about half that for ester dispersed. Furthermore, for water dispersed, there was only a very modest variation of drop size with location throughout the vessel. Under batch conditions it was easily possible to maintain a value of $\overline{\varphi}$ of 0.60, as large as 0.70 under flow conditions. The evidence suggests that the water drops in some manner were stabilized, that is, prevented from coalescing, for reasons not now known.

In the case of water dispersed in isopropyl benzene, it was not possible to maintain a dispersion with the impeller speeds available with our speed reducer.

These and other water-dispersed systems are under further study.

OTHER CORRELATIONS

The other correlations in the literature are for baffled vessels. They were nevertheless tested with the present batch data for unbaffled vessels. The best was that of Bouyatiotis and Thornton (1967), which can describe $\overline{d_p}$ moderately well (average deviation 10 to 17%) for dispersions of octanol, methylamyl acetate, and isopropyl benzene in water, for which the physical properties are in the range studied by them, but which substantially overestimates the drop size (av. deviation 35 to 232%) for cyclohexanone dispersed in water, and for water dispersed in cyclohexanone or in octanol, for which the properties are outside the range they studied. In view of the fact that both their and our correlations depend strongly upon the power dissipation, this supports the idea that baffled and unbaffled vessels may develop approximately the same specific interfacial area when compared at the same power/volume and the same dispersed-phase holdup.

ACKNOWLEDGMENT

We gratefully acknowledge support by the National Science Foundation, under Grants GK-1406 and GK-14007.

NOTATION

a = local specific interfacial area, m²/m³
$\overline{a}$ = vessel-average of a, m²/m³
C_1-C_4, C_6 = dimensionless constants
C_5 = dimensional constant
c_1-c_5, c'_1-c'_9 = constants
D = impeller diameter, m
d_i = diameter of the ith drop, m
d_{max} = maximum drop diameter, m
d_p = local Sauter-mean drop diameter, m
$\overline{d_p}$ = vessel-average of d_p

f_1, f_2 = functions
g = acceleration of gravity, m/s^2
g_c = conversion factor: 1 kg·m/N·s^2; 32.17 (lb.$_m$)·ft/(lb.$_f$)·s^2
H = height of liquid in vessel = height of vessel, m
k_d = wave number characteristic of energy-dissipating eddies, m^{-1}
k_e = wave number characteristic of energy-containing eddies, m^{-1}
L_e = average size of energy-containing eddies, m
N_F = $Q_D\, \rho_C\, \sigma\, g_c/\mu_C^3$, dimensionless
N_G = $\mu_C^4 g/\rho_C\, \sigma^3\, g_c^3$, dimensionless
N_{Pv} = $PQ_D\mu_C^2/V\, \sigma^3 g_c^2$, dimensionless
N_{vis} = $\mu_D/(\rho_D \sigma g_c d)^{0.5}$, dimensionless
N_{We} = a Weber number, $\rho_C \overline{u^2}\, \bar{d}_p/\sigma g_c$, dimensionless
$N_{We,C}$ = a critical value of N_{We}, dimensionless
N_μ = μ_D/μ_C, dimensionless
N_ρ = $\Delta\rho/\rho_C$, dimensionless
N_ϕ = $\bar{\varphi}/x_F$, dimensionless
n_i = number of drops of diameter d_i
P = power input to impeller, $N \cdot m/s$
P_D = rate of energy removal by dispersed phase, N·m/s
Q = flow rate, m^3/s
t = residence time, s
$\overline{u^2}$ = square of root-mean-square turbulent fluctuating velocity over the wave-number range under consideration m^2/s^2
V = vessel volume, m^3
x_F = volume fraction of dispersed liquid in feed mixture = $Q_D/(Q_C + Q_D)$, dimensionless
γ = a dimensional constant
$\Delta\rho$ = absolute value of density difference = $|\rho_C - \rho_D|$, kg/m^3
ϵ = rate of energy dissipation/mass of liquid, m^2/s^3
η = size of energy-dissipating eddies, m
μ = viscosity, N·s/m^2 = kg/m·s
ν = kinematic viscosity, m^2/s
ρ = density, kg/m^3
σ = interfacial tension, N/m
φ = local dispersed-phase holdup, m^3 disp.-phase holdup/m^3 dispersion
$\bar{\varphi}$ = vessel-average of φ, m^3/m^3

Subscripts

C = continuous phase
D = dispersed phase

All equations except Equations (13*a*) to (13*f*) may be used directly with any consistent set of units. Table 6 lists values of c_1 in the coefficient 10^{c_1} of these equations for English units as well as for S. I. units.

TABLE 6. CONSTANTS OF EQUATIONS (13*a*) TO (13*f*)

Equation	c_1 in 10^{c_1} for S. I. units (meters, kilograms, Newtons, sec.)	c_1 in 10^{c_1} for English units (feet, lb. mass, lb. force, seconds)
(13*a*)	−2.316	−1.978
(13*b*)	−2.488	−2.089
(13*c*)	−1.645	−1.432
(13*d*)	−2.066	−1.812
(13*e*)	−2.192	−1.921
(13*f*)	−1.759	−1.558

LITERATURE CITED

Bouyatiotis, B. A., and J. D. Thornton, "Liquid Extraction Operations in Stirred Vessels," *Ind. Chemist,* **39,** 298 (1963).

————., "Liquid-liquid Extraction Studies in Stirred Tanks, Part I: Droplet Size and Holdup Measurements in a Seven-inch Diameter Baffled Vessel," *Inst. Chem. Engrs. (London) Symp. Ser.,* **26,** 43 (1967).

Calderbank, P. H., "Physical Rate Processes in Industrial Fermentation, Part I," *Trans. Inst. Chem. Engrs. (London),* **36,** 443 (1958).

Chen, T. H., and S. Middleman, "Drop-Size Distribution in Agitated Liquid-liquid Systems," *AIChE J.,* **13,** 989 (1967).

Cutter, L. A., "Flow and Turbulence in a Stirred Tank," *ibid.,* **12,** 35 (1966).

Fick, J. L., H. E. Rea, and T. Vermeulen, "The Effects of Agitator Geometry on the Mixing of Liquid-liquid Systems," U.S. Atomic Energy Comm., UCRL-2545 (1954).

Greenfield, H., "Catalytic Hydrogenation of Aromatic Nitro Groups," *Trans. N. Y. Acad. Sci. Ser. III,* **31,** 1038 (1969).

Heisenberg, W., "Zur statistischen Theorie der Turbulenz," *Z. Physik,* **124,** 628 (1948).

Hinze, J. O., "Fundamentals of the Hydrodynamic Mechanism of Splitting Up in Dispersion Processes," *AIChE J.,* **1,** 289 (1955).

Hinze, J. O., *Turbulence,* Ch. 3, McGraw-Hill, New York (1959).

Kawecki, W. T., T. Reith, J. W. Van Heuvan, and W. S. Beck, "Bubble-Size Distribution in the Impeller Region of a Stirred Vessel," *Chem. Eng. Sci.,* **22,** 1519 (1967).

Laity, D. S., and R. E. Treybal, "Dynamics of Liquid Agitation in the Absence of an Air-Liquid Interface," *AIChE J.,* **3,** 176 (1957).

Mack, D. E., and A. E. Kroll, "Effect of Baffles on Agitator Power Consumption," *Chem. Eng. Progr.* **44,** 189 (1948).

Mlyneck, Y., and W. Resnick, "Drop Sizes in Agitated Liquid-liquid Systems," *AIChE J.,* **18,** 122 (1972).

Mok, Y. I., and R. E. Treybal, "Continuous-phase Mass-transfer Coefficients for Liquid Extraction in Agitated Vessels, II," *ibid.,* **17,** 916 (1971).

Overcashier, R. H., H. A. Kingsley, and R. B. Olney, "Liquid Extraction in an Agitated Vessel," *ibid.,* **2,** 529 (1956).

Paul, E. L., and R. E. Treybal, "Mixing and Product Distribution for a Liquid-phase, Second-order, Competitive-consecutive Reaction," *ibid.,* **17,** 718 (1971).

Rea, H. A., and T. Vermeulen, "Effect of Baffling and Impeller Geometry on Interfacial Area in Agitated, Two-phase Liquid Systems," U.S. Atomic Energy Comm. UCRL-2123 (1953).

Rodger, W. A., "Interfacial Area in Liquid-liquid Dispersions Related to Fluid Motion in Mixing Vessels," U.S. Atomic Energy Comm. ANL-5575 (1956).

Rodger, W. A., V. G. Trice, and J. H. Rushton, "Effect of Fluid Motion on Interfacial Area of Dispersions," *Chem. Eng. Progr.,* **52,** 515 (1956).

Rushton, J. H., "The Use of Pilot-Plant Mixing Data," *ibid.,* **47,** 485 (1951).

Schindler, H. D., and R. E. Treybal, "Continuous-phase Mass-transfer Coefficients for Liquid Extraction in Agitated Vessels," *AIChE J.,* **14,** 790 (1968).

Schwartzberg, H. G., and R. E. Treybal, "Fluid and Particle Motion in Turbulent Stirred Tanks," *Ind. Eng. Chem. Fundamentals,* **7,** 1, 6 (1968).

Sprow, F. B., "Distribution of Drop Sizes Produced in Turbulent Liquid-liquid Dispersions," *Chem. Eng. Sci.,* **22,** 435 (1967).

————., "Drop-Size Distributions in Strongly Coalescing, Agitated Liquid-liquid Systems," *AIChE J.,* **13,** 995 (1967).

Sullivan, D. M., and E. E. Lindsay, "An Approach to Characterizing Agitation by Dispersion Particle Size," *Ind. Eng. Chem. Fundamentals,* **1,** 87 (1962).

Treybal, R. E., *Liquid Extraction,* 2nd ed., p. 411, McGraw-Hill, New York (1963).

Trice, V. G., and Rodger, W. A., "Light Transmittance as a Measure of Interfacial Area," U.S. Atomic Energy Comm. ANL-5512 (1956).

Weinstein, B. "Mixing Characteristics for Liquid Extraction in Unbaffled Vessels," Ph.D. dissertation, New York University (1972).

Manuscript received June 29, 1972; revision received October 5, 1972; paper accepted October 6, 1972.